ELSEVIER

Chemical Geology 181 (2001) 147–167

CHEMICAL GEOLOGY
INCLUDING
ISOTOPE GEOSCIENCE

www.elsevier.com/locate/chemgeo

The altitude effect on the isotopic composition of tropical rains

Roberto Gonfiantini [a,*], Michel-Alain Roche [1], Jean-Claude Olivry [b], Jean-Charles Fontes [2], Gian Maria Zuppi [c]

[a] *Istituto di Geocronologia e Geochimica Isotopica del CNR, Area della Ricerca di Pisa, Via G. Moruzzi 1, 56124 Pisa, Italy*
[b] *Institut de Recherche pour le Développement, Montpellier, France*
[c] *Dipartimento di Scienze Ambientali, Università Ca' Foscari, Venice, Italy*

Received 11 September 2000; accepted 1 March 2001

Abstract

Data on the Isotopic composition of yearly and monthly precipitation samples collected at various altitudes on Mount Cameroon, Africa, and in two transects from the Amazon to the Altiplano in Bolivia, South America, are presented. In Bolivia, the $^{2}H/^{1}H$ and $^{18}O/^{16}O$ ratios show seasonal variations, with lower values in the summer rainy months with respects to the winter dry ones. The $\delta^{2}H$ and $\delta^{18}O$ values are linearly correlated with a slope of 7.5 in all seasons, but the intercept is higher in winter than in summer.

The δ-gradient vs. altitude is larger in rainy periods. The isotopic data are fitted by using a numerical model based on Rayleigh adiabatic condensation process. Model simulations show that the δ–altitude relationship slightly deviates from linearity, because the slope increases with altitude due to the lowering of temperature and the consequent increase of the condensation rate of atmospheric vapour. The parameters which most affect the shape of δ–altitude relationships are the temperature vertical gradient (lapse rate) and the initial relative humidity of the ascending air masses, while a change of the initial isotopic composition of water vapour determines a shift of the curve along the δ-axis. In addition, the model explains the observed increase of the deuterium excess with altitude.

Keywords: Altitude effect; Hydrogen isotopes; Oxygen isotopes; Precipitation; Rayleigh condensation

1. Introduction

It is well known that the hydrogen and oxygen heavy isotope contents of rainwater decrease with increasing altitude. This is attributed to the progressive condensation of atmospheric vapour and rainout of the condensed phase, which take place when air masses climb up along the slopes of high mountains and cool off as a consequence of adiabatic expansion. As the $^{2}H/^{1}H$ and $^{18}O/^{16}O$ ratios are slightly higher in the liquid water or ice removed by precipitation than in the residual vapour, the latter becomes progressively depleted in heavy isotopes.

In this paper, we report and discuss the excellent examples of altitude effect on the isotopic composition of precipitation observed in stations from sea level to the top of Mount Cameroon, Africa, and in two transects from the Bolivian Amazon up to the

* Corresponding author. Tel.: +39-050-315-2358; fax: +39-050-315-2360.
E-mail address: R.Gonfiantini@iggi.pi.cnr.it (R. Gonfiantini).
[1] Present address: 1, Cour de la Commanderie, 17000 La Rochelle, France.
[2] Formerly at Laboratoire d'Hydrologie et de Géochimie Isotopique, Université de Paris Sud, Orsay, France.

0009-2541/01/$ - see front matter
PII: S0009-2541(01)00279-0

Altiplano, South America. The data are discussed in terms of a Rayleigh condensation process.

The precipitation samples were collected and analysed several years ago at the instigation of Jean-Charles Fontes. The data were partly presented and discussed by Fontes and Olivry (1976, 1977), Gonfiantini (1998) and Roche et al. (1999). However, most of the data are published and discussed here in detail for the first time, as well as the model elaboration presented in Appendix A.

2. Precipitation regime and sampling sites

2.1. Mount Cameroon

Mount Cameroon is an isolated ancient volcano in proximity of the Atlantic coast in Equatorial Africa, whose peak (4°13′N, 9°10′E) reaches the altitude of 4095 m asl. The humid air masses coming from the ocean climb up along the mountain slopes and produce precipitation. Rains are very abundant in coastal stations: for instance, a mean value of 9895 mm $year^{-1}$ over 38 years has been recorded at Debundscha (Station 17 in Table 1), with a maximum value of 14,694 mm in 1919 (Fontes and Olivry, 1977). The precipitation decreases with increasing altitude and distance from the sea.

Information on long-term mean monthly temperature and amount of precipitation are available in WMO records for several meteorological stations in Cameroon (WMO/OMM, 1996). The closest station to Mt. Cameroon is Douala Observatoire (4°00′N and 9°44′E, 9 m asl) located 65 km southeast of the mountain peak. The mean precipitation in Douala is 3854 mm $year^{-1}$, with monthly values ranging from 755 mm in August to less than 40 in December and January. Thus, 75% of precipitation falls from June to October. The mean air temperature is 26.7°C, with monthly values ranging from 24.9°C in August, the most rainy month, to 28.1 in February. The mean relative humidity is 88% in the full rainy season and drops to 80% in the dry season. The mean vertical gradient of air temperature, measured by radio balloons, is -5.3°C km^{-1} and it is practically constant throughout the year (Fontes and Olivry, 1977).

Yearly precipitation samples were collected during a 4-year period (1972–1975) at 20 stations with

Table 1
Mount Cameroon: station altitude, distance from the Atlantic Ocean, and amount of precipitation.

No.	Station	Altitude (m asl)	Distance from the ocean (km)	Amount of precipitation (mm)				
				1972	1973	1974	1975	Mean
16	Bakingele	10	0.6	7930	5365	6785	6565	6661
17	Debundscha	20	0.8	9200	8430	8015	8350	8499
19	Idenau	30	2.5	7915	6870	7530	7140	7364
15	Batoki	50	1.0	6130	4590	5295	5115	5283
22	Brasseries	180	10.5	4455	1990	2700	2150	2824
20	Bomana	460	11	5525	5050		5870	5482
25	Bonakanda	860	21.5	3730	2990	3225	3140	3271
14	Forêt SW	1000	8.5	7210	4810	8735	8290	7261
23	Upper Farm	1100	17	3730	2210	2725	2665	2833
6	Route VHF	1610	25	4070	2850	3175	3515	3403
13	Limite Forêt SW	2320	13	3945	2270	2825	3240	2759
4	Station VHF	2460	28	3945	2270	2825	3240	2759
7	Versant Nord	2475	29	3050	2600	1950	3425	2756
3	Versant Nord	2500	28	3315	2735	3050	3125	3056
24	Limite Forêt BUEA	2500	20	3800	2680	3075	3200	3189
9	Hutte 2	2925	21	3120	2310	2725	3050	2801
12	Versant SW	3000	16	3030	1830	2475	2900	2559
8	Nord	3050	26	2480	1900	2025	2725	2283
11	Southwest	3300	19	2100	1400	1550	2075	1781
10	Sommet Bottle Peak	4050	22	2540	1875	2150	2300	2216

elevation ranging from 0 to 4050 m asl (Fig. 1). Paraffin oil was added to the rain water containers in order to prevent evaporation during rain collection. The station main characteristics and the yearly amount of precipitation are shown in Table 1.

During the sampling period, the main climatological parameters showed variations within the normal range. However, it may be worth to underline that the precipitation amount was about 20% below average in 1972 and 1973, during which the Sahelian belt of Northern Africa was affected by a severe drought.

2.2. Bolivia

The precipitation samples were collected in stations along two transects between the latitudes 14°30′ and 17°30′S and the longitudes 64°30′ and 68°W, as shown in Fig. 2. The main characteristics of sampling sites are reported in Tables 2 and 3.

The first transect Yungas–Altiplano (12 stations) starts at Trinidad (200 m) and Rurrenabaque (300 m asl) in the Amazon basin of Bolivia and reaches the Altiplano at El Alto (4080 m), after crossing the Andean Eastern Cordillera at Chacaltaya (5200 m). Monthly precipitation samples were collected in the period December 1982 to December 1984, and more irregularly from then till April 1986. Some samples were lost due to logistic difficulties in running remote stations.

The second transect Chaparé–Cochabamba starts at Villa Tunari and Puerto Villaroel (400 m asl) in the Amazon, rises to Corani (3200 m) through the Chaparé valley, then descends to Cochabamba (2560 m). Annual samples were collected in 1984 and 1985 by using paraffin oil to prevent evaporation.

Under the influence of northeastern and south eastern trade winds, the air masses reach the Andes foothill from the Atlantic Ocean after crossing the

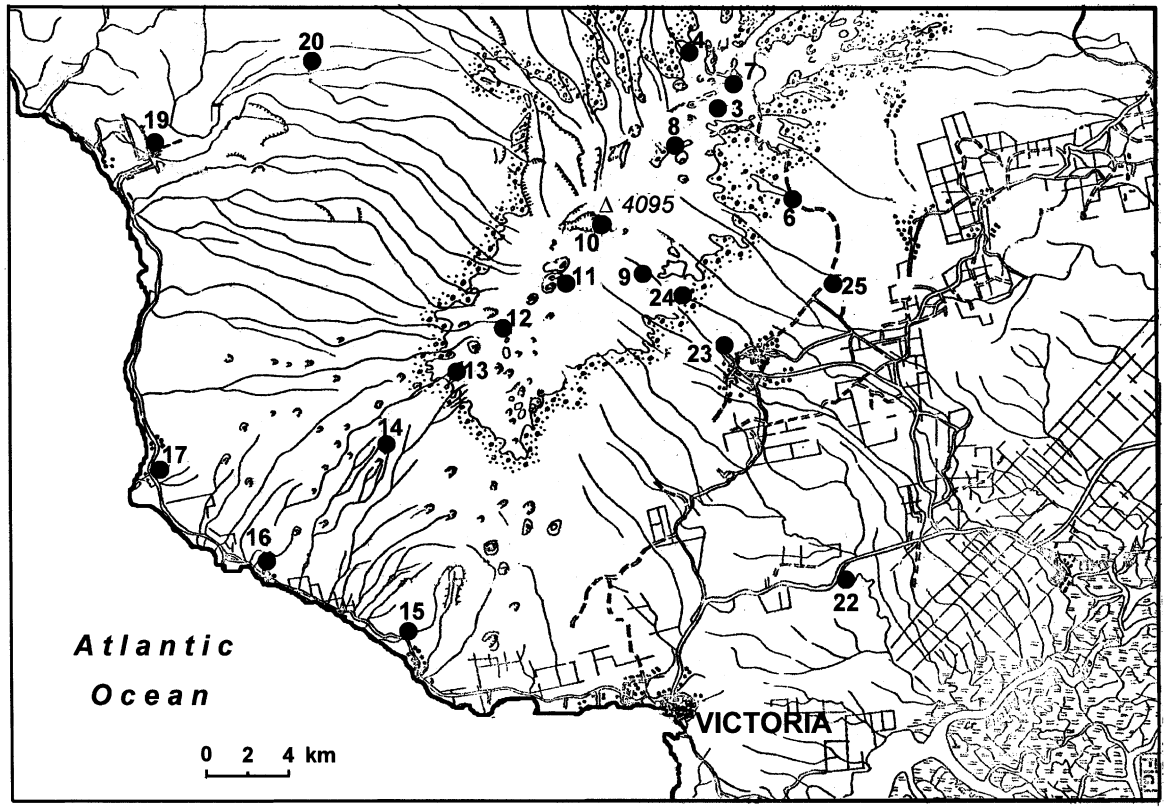

Fig. 1. Mt. Cameroon, western equatorial Africa. Location of sampling stations. The peak (4090 m asl) coordinates are: 4°13′N and 9°10′E.

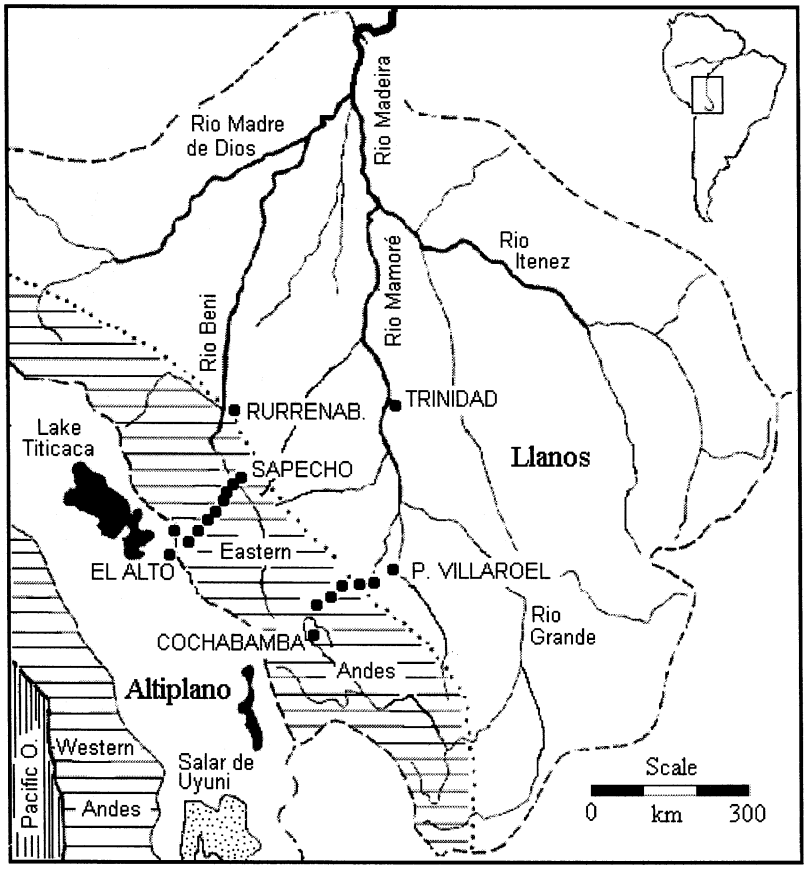

Fig. 2. Bolivia. Location of sampling transects at latitude between 14°30′ and 17°30′S and longitude between 64°30′ and 68°W.

Amazon basin and the northern part of the Rio de La Plata basin. The rise of these warm and humid air masses over the Andes produces precipitation in the region between the upper valley of Rio Madeira and the Western Cordillera, which feeds the run-off into the Amazon basin and the Lake Titicaca (Ronchail, 1989; Roche et al., 1992). The air mass trajectory, driven by the seasonal displacement of the intertropical convergence zone, is occasionally perturbed by the intrusion of a southern cold front which may reach the Bolivian territory and produce rains at the contact with the easterly warm and humid air masses.

The precipitation amount decreases from 2000 to 3000 mm year^{-1} on the Andean Piedmont, where values up to 6000–7000 mm year^{-1} are occasionally recorded, to less than 500 over most of the altiplano (Roche and Fernandez, 1988; Roche and Rocha, 1985). This trend is determined by the orography and the Southern Pacific anticyclone. The spatial distribution of precipitation may show local deviations due to the influence of the Lake Titicaca and the Uyuni and Coipaxa salt lakes (salares).

The seasonal distribution of precipitation is similar all over the region. The rainy season extends from December to March, and the (relatively) dry season from May to September.

In 1982–1983 El Niño Southern Oscillation (ENSO) was particularly enhanced in eastern equatorial Pacific, and caused abundant rains in Ecuador and Northern Peru (Ardanuy et al., 1987; Goldberg et al., 1987). On the contrary, the 1983 precipitation over the Bolivian and Peruvian Altiplano south of 15°S was less than the half of the normal amount, as recorded by ORSTOM and NOAA (NOAA (Na-

Table 2
Station altitude, temperature, and amount of precipitation in Yungas–Altiplano Transect, Bolivia

No.	Station	Altitude (m asl)	Mean temperature (°C)	1983		1984	
				Mean temperature (°C)	Precipitation (mm)	Mean temperature (°C)	Precipitation (mm)
1	Trinidad	200		24.7 (9)	1563 (9)		
2	Rurrenabaque	300	25.8		2538 (12)		
3	Sapecho	395	24.8	25.2 (12)	1330 (12)	25.7 (11)	1829 (11)
4	Caranavi	600	21.4		1241 (12)	23.2 (11)	1885 (11)
5	Choro	790					
6	Coroico	1700	19.1		1676 (12)	20.7 (11)	2018 (11)
7	Sacramento	2200					
8	Chuspipata	3100					
9	Pongo	4040					
10	La Cumbre	4650					
11	Chacaltaya	5200	−0.8		442 (12)		600 (10)
12	El Alto	4080	8.2	7.5 (12)	424 (12)		703 (9)

N.B.: Number of monthly data are available in brackets.

tional Oceanic and Atmospheric Administration), 1983, 1984). In the 1983–1984 rainy season, which was not affected by El Niño, the precipitation was exceptionally high. However, during the recent 1997–1998 El Niño event, which was more intense than in 1982–1983, no drought occurred in the Lake Titicaca basin (Gaita, 1999). Therefore, the influence of El Niño on precipitation on the southern part of the Altiplano is not proved.

The seasonal excursion of the mean monthly surface temperature is about 5°C in all the stations, with the maximum temperature recorded in November–December and the minimum in the dry months of July–August. Another secondary minimum occurs in the rainy season: for instance, in 1984 the mean temperature was about the same in January–February and in July–August, i.e. 7–8°C at El Alto on the Altiplano, and 25–26°C at Rurrenabaque in the Amazon. But in January–February 1983, when rains were scarce, the mean temperature was 11°C at El Alto and 28–29°C at Rurrenabaque (NOAA (National Oceanic and Atmospheric Administration), 1983, 1984).

At ground level, the temperature gradient vs. altitude is approximately -5.0°C km^{-1}, as derived from stations in both transects. This gradient is similar to that observed in Ecuador (-4.9°C km^{-1}, computed from García et al., 1998), and to the air

Table 3
Station altitude, temperature, amount and δ^{18}O of annual precipitation in Chaparé–Cochabamba Transect, Bolivia

No.	Station	Altitude (m asl)	Mean temperature (°C)	1984		1985	
				Precipitation (mm)	δ^{18}O (‰)	Precipitation (mm)	δ^{18}O (‰)
1	Puerto Villaroel	405	23.2	3000	−7.42	1798	−7.48
2	Villa Turani	470	24.7	5800	−9.10	3442	−6.55
3	Palmar Pampa	820	22.1		−10.00		
4	Santa Isabel	2145	15.1		−13.27		
5	Planta Corani	2600	12.6	3418	−13.69	1585	−10.18
6	Presa Corani	3220	9.3	3030	−14.60	1495	−11.63
7	Cochabamba	2560	18.1	706	−16.24	567	−10.46

vertical gradient measured in Cameroon (-5.3‰ km^{-1}, see Section 2.1). Cochabamba, due to its position, enjoys a temperature about 5°C higher than other stations at the same altitude. Data from stations in the Amazon Basin indicate that the relative humidity is 85–90% in January and 80–85 in July.

3. Isotope measurements

The oxygen isotope measurements were carried out at the Laboratoire de Géologie Dynamique, Université de Paris-VI for the Mount Cameroon samples, and at the Laboratoire de Géochimie et d'Hydrologie Isotopique, Université de Paris-Sud, Orsay, for the Bolivian samples. The hydrogen isotope measurements, carried out on part of the samples only, were performed at the Commissariat à l'Energie Atomique, Saclay. As usual, the isotopic composition is expressed in δ per mil, i.e. deviation ‰ of the isotope ratios $^{2}H/^{1}H$ and $^{18}O/^{16}O$ from the reference V-SMOW. The isotopic data are reported in Tables 3–6.

The isotopic composition of some samples may be affected by evaporation, as deduced from the deuterium excess (defined as $d = \delta^{2}H - 8\delta^{18}O$, Dansgaard, 1964). They are: October 1983 at Rurrenabaque, March 1983 at Sapecho, and August and September 1983 at Sacramento (cf. Table 6). This may be due to poor storage or improper sampling procedure, but, for samples collected during the dry season, may be due as well to evaporation affecting the raindrops during the fall. Finally, there are doubts about the January 1983 sample from Chuspipata, whose δ values are not consistent with those obtained in other stations.

4. The $\delta^{18}O$–$\delta^{2}H$ relationship

The $\delta^{18}O$–$\delta^{2}H$ orthogonal regression for Cameroon, from the 18 data pairs available, is:

$$\delta^{2}H = (7.39 \pm 0.21)\,\delta^{18}O + (4.9 \pm 1.4) \qquad (1)$$

The slope of Eq. (1), less than 8, reflects the fact that the deuterium excess increases with altitude, i.e.

Table 4
Mount Cameroon. Isotopic composition of yearly precipitation

No.	Station	1972		1973		1974	1975	Mean
		$\delta^{18}O$ (‰)	$\delta^{2}H$ (‰)	$\delta^{18}O$ (‰)	$\delta^{2}H$ (‰)	$\delta^{18}O$ (‰)	$\delta^{18}O$ (‰)	$\delta^{18}O$ (‰)
16	Bakingele	−2.41	−12.4	−2.93	−17.5	−3.36	−3.38	−3.02
17	Debundscha	−2.61		−3.09		−3.67	−3.33	−3.18
19	Idenau	−3.02		−3.59	−25.4	−3.87	−3.82	−3.58
15	Batoki	−2.45		−2.92		−3.28	−3.69	−3.08
22	Brasseries	−3.26		−3.61	−24.1	−3.86	−4.08	−3.70
20	Bomana	−3.58		−3.94		−4.05	−3.96	−3.88
25	Bonakanda	−4.19		−4.73		−4.86	−4.88	−4.66
14	Forêt SW	−3.62	−22.8	−4.86		−4.25	−4.17	−4.22
23	Upper Farm	−4.39	−26.2	−4.94	−29.2	−5.06	−5.59	−5.00
6	Route VHF	−5.74	−34.7	−5.98		−5.75	−4.94	−5.60
13	Limite Forêt SW	−6.13		−6.90		−8.61	−7.07	−7.18
4	Station VHF	−6.38		−6.99	−46.5	−7.04	−7.19	−6.90
7	Versant Nord	−6.25		−6.56		−5.85	−6.71	−6.34
3	Versant Nord	−6.59	−44.6	−7.44		−7.24	−6.99	−7.06
24	Limite Forêt BUEA	−6.25	−36.3	−6.29	−43.1	−6.74	−7.01	−6.57
9	Hutte 2	−7.57	−49.6	−7.50		−7.93	−7.39	−7.60
12	Versant SW	−7.38		−8.22	−55.4	−8.92	−7.55	−8.02
8	Nord	−7.53		−8.28		−8.33	−7.92	−8.02
11	Southwest	−8.44	−59.2	−8.98	−62.6	−9.11	−8.24	−8.69
10	Sommet Bottle Peak	−8.89	−61.1	−9.77	−68.0	−9.95	−9.45	−9.52

Table 5
Altitude of sampling stations in the Yungas–Altiplano Transect and mean weighted and unweighted $\delta^{18}O$ values

No.	Station	All values		1983			1984		
		$\delta^{18}O$ (‰) unweighted	n	$\delta^{18}O$ (‰) unweighted	$\delta^{18}O$ (‰) weighted	n	$\delta^{18}O$ (‰) unweighted	$\delta^{18}O$ (‰) weighted	n
1	Trinidad	−3.84	15						
2	Rurrenabaque	−5.10	16	−3.4	−2.87	10			
3	Sapecho	−6.29	31	−4.7	−3.46	10	−9.5	−7.77	11
4	Caranavi	−6.66	29	−4.2	−3.54	12	−10.4	−8.85	11
5	Choro	−6.40	30		−3.68	12		−9.29	11
6	Coroico	−7.80	28	−3.9	−4.36	12	−11.7	−10.68	11
7	Sacramento	−8.07	28		−5.13	12		−10.85	11
8	Chuspipata	−9.61	28		−6.56	12		−12.82	10
9	Pongo	−11.93	28		−8.81	12		−14.77	9
10	La Cumbre	−12.87	24		−8.32	10		−17.60	9
11	Chacaltaya	−13.86	27	−11.7	−10.54	12	−20.4	−17.65	10
12	El Alto	−12.39	27	−8.1	−8.55	11	−18.5	−15.75	10

N.B. Mean yearly values have been derived when at least 10 monthly values were available.

with decreasing δ values. This is also observed in the Yungas–Altiplano transect in Bolivia, where the mean deuterium excess is 17.8 ± 0.4‰ for stations with altitude above 4000 m asl, 16.4 ± 0.5 for stations between 4000 and 1000 m asl, and 9.5 ± 0.7 for station at lower altitude.

Seasonal $\delta^{18}O$–$\delta^{2}H$ relationships can be derived for the Yungas–Altiplano transect. For the exceptionally rainy months of January and February 1984, the regression is:

$$\delta^{2}H = (7.48 \pm 0.16)\,\delta^{18}O + (5.1 \pm 2.7) \qquad (2)$$

For January–February 1983, severely affected by drought, the relationship has the same slope but a higher intercept:

$$\delta^{2}H = (7.45 \pm 0.33)\,\delta^{18}O + (9.1 \pm 2.9) \qquad (3)$$

For July–September 1983, i.e. the months of the dry season with the highest δ values, the relationship has again about the same slope, but a even higher intercept:

$$\delta^{2}H = (7.50 \pm 0.27)\,\delta^{18}O + (16.3 \pm 0.9) \qquad (4)$$

Eqs. (2)–(4) show that the spatial $\delta^{18}O$–$\delta^{2}H$ relationships shifts seasonally, by changing intercept but keeping the same slope.

In the tropics, however, winter rains are enriched in heavy isotopes with respect to the summer ones, because the amount effect is the main isotopic driving factor (see next section). Thus, by combining summer rains with low intercept and winter rains with high intercept, the resulting slope must be higher than those of the seasonal relationships (2), (3) and (4). By using all 132 monthly data pairs available for the Altiplano–Yungas transect, the relationship is in fact (Fig. 3):

$$\delta^{2}H = (8.01 \pm 0.08)\,\delta^{18}O + (15.2 \pm 0.7) \qquad (5)$$

The slope of Eq. (5) coincides with that computed by Craig (1961) for natural waters not submitted to evaporation, and confirmed by Dansgaard (1964) and Rozanski et al. (1993). The slope lower than 8 obtained for Cameroon reflects the fact that Eq. (1) represents basically the rain season only, because rainy months largely prevail in determining the yearly means.

It is interesting to compare the above $\delta^{18}O$–$\delta^{2}H$ seasonal relationships with those obtained at latitudes between 30° and 60°. Using mean monthly data published by IAEA (International Atomic Energy Agency) (1992) the regression for July (January in the southern hemisphere) is:

$$\delta^{2}H = (8.33 \pm 0.13)\,\delta^{18}O + (8.2 \pm 3.9) \qquad (6)$$

and for January (July in the southern hemisphere):

$$\delta^{2}H = (8.36 \pm 0.13)\,\delta^{18}O + (14.2 \pm 3.9) \qquad (7)$$

The intercept difference, with virtually identical slope, is attributed to changing conditions at the source of atmospheric moisture.

Table 6
Monthly values in the Yungas–Altiplano Transect, Bolivia

Month	1—Trinidad			2—Rurrenabaque				3—Sapecho					4—Caranavi				
	T (°C)	mm	$\delta^{18}O$	mm	$\delta^{18}O$	$\delta^{2}H$	d	T (°C)	mm	$\delta^{18}O$	$\delta^{2}H$	d	T (°C)	mm	$\delta^{18}O$	$\delta^{2}H$	d
Dec. 1982	26.9	297.5	−11.31	267.0				25.8	145.7				24.1	92.4	−7.41	−53.1	6.2
Jan. 1983	27.4	531.7	−4.97	199.0	−4.68	−32.7	4.7	26.4	205.0	−6.04	−38.8	9.5		191.0	−3.98	−17.7	14.1
Feb. 1983	27.2	178.1	−4.85	408.0	−4.76	−30.7	7.4	26.8	306.7	−6.21	−38.8	10.9		210.0	−6.79	−43.8	10.5
Mar. 1983	27.1	182.7	−5.64	168.0				26.3	94.9	−7.42	−59.0	0.4		129.0	−7.03	−47.4	8.8
Apr. 1983	26.8	116.8	−6.39	243.0	−7.32	−47.6	11.0	26.3	257.4	−4.22	−23.1	10.7		44.7	−6.46	−46.9	4.8
May 1983	24.6	345.6	−3.16	404.0				25.1	156.4	−0.67	6.3	11.7		77.0	−4.05	−23.1	9.3
Jun. 1983	18.2	7.1	−1.25	198.0	−0.93	3.0	10.4	21.5	34.8	1.47	22.4	10.6		58.8	−1.98	−3.5	12.3
Jul. 1983	22.1	71.0	1.25	249.0	1.08	22.0	13.4	22.7	84.0					94.0	0.81	19.0	12.5
Aug. 1983	23.3	1.6	0.62	24.0	−0.66	8.2	13.5	24.7	0.8	0.27	12.7	10.5		35.5	1.21	23.5	13.8
Sep. 1983				78.0	1.66	24.6	11.3	24.8	47.2	−1.33	3.9	14.5		85.4			
Oct. 1983	25.3	128.1	−0.67	236.0	−0.83	−9.1	−2.5	26.0	51.4					81.2	−2.87	−10.2	12.8
Nov. 1983				166.0	−5.03	−34.3	5.9	26.0	35.8	−3.40	−17.4	9.8		107.0	−5.90	−38.3	8.9
Dec. 1983				164.6	−7.25			25.8	55.9	−7.01	−47.8	8.3		127.5	−5.46	−32.1	11.6
Jan. 1984				349.4	−9.65			25.9	373.3	−7.58	−50.5	10.1	24.2	389.0	−9.59	−68.6	8.1
Feb. 1984				468.0	−10.05			26.4	216.5	−11.99			22.9	314.5	−13.81	−108.2	2.3
Mar. 1984				129.8	−10.07			26.7	190.7	−11.52			22.8	380.5	−12.58		
Apr. 1984								26.0	290.1	−13.32			22.9	158.6	−12.69		
May 1984				91.8	−7.60			25.4	83.1	−8.50			22.6	18.4	−9.71		
Jun. 1984								23.8	45.1	−2.52			23.4	5.0	−4.62		
Jul. 1984								23.5	76.7	−2.93							
Aug. 1984													21.4	60.5	−1.12		
Sep. 1984								25.0	32.3	−2.73			24.3	148.3	−6.24		
Oct. 1984								27.0	86.8	−5.91			23.9	145.6	−5.60		
Nov. 1984								26.2	282.1	−10.42			23.0	177.0	−10.64		
Dec. 1984								27.3	151.9	−8.08			24.4	88.0	−10.73		
Jan. 1985				328.0	−7.64			26.4	155.7	−8.65							
Feb. 1985				268.0	−7.82			27.0	123.0	−9.72			22.2	152.0	−10.51		
Mar. 1985	26.7	246.1	−5.47					26.9	196.5	−9.80			26.6	237.5	−11.12		
Apr. 1985	24.7	205.5	−7.23					25.8	175.7	−6.39							
May 1985	24.9	21.5	−6.30														
Jun. 1985	21.7	6.2	−1.38					22.8	16.1	−2.72			22.4	15.0	−9.83		
Jul. 1985	21.9	148.7	−0.89														
Dec. 1985								27.4	89.6	−6.57				180.5	−3.28		
Jan. 1986								26.6		−8.65							
Feb. 1986										−9.72							
Mar. 1986										−9.80					−11.12		
Apr. 1986										−2.79							

Month	5—Choro	6—Coroico					7—Sacramento			8—Chuspipata		
	$\delta^{18}O$	T (°C)	mm	$\delta^{18}O$	$\delta^{2}H$	d	$\delta^{18}O$	$\delta^{2}H$	d	$\delta^{18}O$	$\delta^{2}H$	d
Dec. 1982	−4.61		186.2	−7.01						−7.52		
Jan. 1983	−6.76	23.2	186.5	−6.28	−35.0	15.2	−6.76	−39.2	14.9	−12.64	−97.1	4.0
Feb. 1983	−5.90	21.9	192.8	−6.52	−37.7	14.5	−7.10	−41.5	15.3	−8.13	−48.0	17.0
Mar. 1983	−7.17		143.4	−6.64	−40.0	13.1	−7.68	−45.6	15.8	−8.95	−55.3	16.3
Apr. 1983	−6.02	23.0	25.8	−7.34	−47.0	11.7	−8.07	−50.2	14.4	−9.26	−56.3	17.8
May 1983	−4.69	21.0	125.6	−7.12	−40.8	16.2	−8.17	−49.9	15.5	−9.12	−55.9	17.1
Jun. 1983	−2.13	19.2	103.2	−3.78	−14.6	15.6	−4.10	−16.5	16.3	−5.40	−25.6	17.6
Jul. 1983	0.58	19.6	235.0	−0.55	14.1	18.5	−1.71	4.6	18.3	−2.58	−2.3	18.3
Aug. 1983	0.64	19.2	180.0	0.29	20.5	18.2	−1.34	−11.2	−0.5	−2.00	5.9	21.9
Sep. 1983	0.37		164.8	−0.90	11.1	18.3	0.24	−21.7	−23.6	−3.21	−5.2	20.5
Oct. 1983	−2.47		81.3	−2.52	−4.3	15.9	−4.01	−14.0	18.1	−4.15	−12.3	20.9
Nov. 1983	−5.34		117.3	−7.29	−40.7	17.6	−7.00	−39.9	16.1	−7.05	−37.6	18.8
Dec. 1983	−5.24		140.6	−3.69	−12.5	17.0	−5.82	−27.6	19.0	−6.27	−29.1	21.1
Jan. 1984	−9.69	20.6	439.6	−11.50	−79.8	12.2	−12.16	−83.0	14.3	−13.82	−96.5	14.1
Feb. 1984	−15.41	20.8	343.9	−15.85	−115.5	11.3	−15.24	−109.0	12.9	−17.33	−124.5	14.1
Mar. 1984	−13.58	21.4	328.5	−15.07			−15.01			−16.98		
Apr. 1984	−13.32	20.8	39.6	−14.82			−14.36			−17.39		
May 1984	−10.36	20.8	16.0	−11.30			−11.33			−13.07		
Jun. 1984	−4.98	19.3	31.0	−6.09			−5.90			−7.88		
Jul. 1984												
Aug. 1984	−2.14	18.8	184.0	−3.68			−4.41			−5.12		
Sep. 1984	−8.05	20.4	65.6	−7.49			−7.56					
Oct. 1984	−0.43	21.7	202.8	−6.71			−6.26			−7.36		
Nov. 1984	−10.67	21.5	264.0	−12.61			−13.37			−14.72		
Dec. 1984	−9.68	21.4	102.5	−12.48			−13.73			−14.48		
Mar. 1985	−9.56	22.1	536.0	−12.31			−11.35			−12.82		
Jun. 1985	−2.46	19.3	5.0	−9.39			−9.86			−11.35		
Aug. 1985	−7.12						−3.61			−4.37		
Nov. 1985							−8.93			−9.80		
Dec. 1985	−5.34	21.9	305.0	−7.53								
Mar. 1986	−0.96	21.0		−12.31			−11.35			−16.28		

(continued on next page)

Table 6 (*continued*)

Month	9—Pongo			10—La Cumbre			11—Chacaltaya				12—El Alto				
	$\delta^{18}O$	$\delta^{2}H$	*d*	$\delta^{18}O$	$\delta^{2}H$	*d*	mm	$\delta^{18}O$	$\delta^{2}H$	*d*	*T* (°C)	mm	$\delta^{18}O$	$\delta^{2}H$	*d*
Dec. 1982							85.0				9.0	46.9	−7.92		
Jan. 1983	−10.09	−63.8	16.9	−10.84	−66.1	20.6	85.0	−10.84	−66.8	19.9	9.4	64.2	−10.53	−69.3	14.9
Feb. 1983	−10.93	−70.9	16.5	−12.62	−82.6	18.4	108.0	−13.07	−86.7	17.9	8.9	35.5			
Mar. 1983	−14.34	−100.8	13.9	−7.50	−44.7	15.3	40.0	−22.44	−164.1	15.4	9.8	24.4	−17.50	−126.9	13.1
Apr. 1983	−12.20	−82.8	14.8				43.0	−13.94	−96.2	15.3	8.6	56.4	−12.55	−84.6	15.8
May 1983	−12.51	−84.0	16.1				28.5	−11.73	−74.5	19.3	6.3	30.8	−11.47	−72.5	19.3
Jun. 1983	−12.55	−85.1	15.3	−11.94	−84.9	10.6	4.3	−11.37	−77.0	14.0	4.7	7.9	−7.39	−44.9	14.2
Jul. 1983	−5.77	−30.8	15.4	−6.51	−36.7	15.4	9.6	−5.81	−35.6	10.9	5.0	8.6	−6.07	−30.7	17.9
Aug. 1983	−2.84	−2.1	20.6	−4.09	−13.1	19.6	13.0	−4.88	−19.2	19.8	5.9	19.6	−4.56	−17.4	19.1
Sep. 1983	−3.41	−4.7	22.6	−4.48	−17.6	18.2	33.0	−5.38	−18.6	24.4	6.7	45.4	−4.80	−13.9	24.5
Oct. 1983	−4.79	−18.2	20.1	−5.95	−29.4	18.2	10.2	−6.21	−30.0	19.7	7.7	24.1	−6.06	−26.1	22.4
Nov. 1983	−9.46	−56.0	19.7	−11.53	−76.3	15.9	15.0	−12.10	−77.1	19.7	8.6	14.0	−6.76	−36.1	18.0
Dec. 1983	−6.82	−31.0	23.6	−7.77	−40.2	22.0	52.8	−8.15	−43.7	21.5	8.2	92.8	−6.41	−29.9	21.4
Jan. 1984	−16.23	−114.9	14.9	−17.18	−120.5	16.9	156.9	−17.88	−125.8	17.2	6.2	183.2	−17.25	−121.3	16.7
Feb. 1984	−21.03	−152.9	15.3	−23.34	−168.6	18.1	161.7	−25.20	−182.4	19.2	6.3	176.8	−23.18	−170.8	14.6
Mar. 1984	−20.33			−21.72			94.9	−24.00			6.9	127.0	−21.73		
Apr. 1984	−20.96			−20.34			24.0	−20.48			6.6	14.4	−18.83		
May 1984				−15.22			2.7	−15.96							
Jun. 1984	−9.66						5.7	−15.28			4.7	9.3	−11.52		
Jul. 1984	−11.76														
Aug. 1984	−6.58			−8.17			9.9	−9.66			4.3	17.5	−9.71		
Sep. 1984	−8.63												−10.46		
Oct. 1984				−12.53			35.9	−10.92			7.9	36.6	−10.46		
Nov. 1984				−19.13			61.1	−16.78				60.9	−16.85		
Dec. 1984	−17.75			−20.75			47.2	−20.29				77.3	−17.52		
Mar. 1985	−16.28			−18.72			70.1	−18.95			7.8	102.2	−18.29		
Apr. 1985	−15.00														
Jun. 1985	−13.34			−8.65			15.8	−16.61				15.8	−17.71		
Aug. 1985	−5.92			−6.07			5.0	−2.73				7.6	−7.57		
Nov. 1985	−13.62			−15.02											
Dec. 1985							95.7	0.00	1.0		7.2	145.2	−13.15		
Mar. 1986	−16.28			−18.72				−18.95			8.5		−18.29		
Apr. 1986	−15.00														

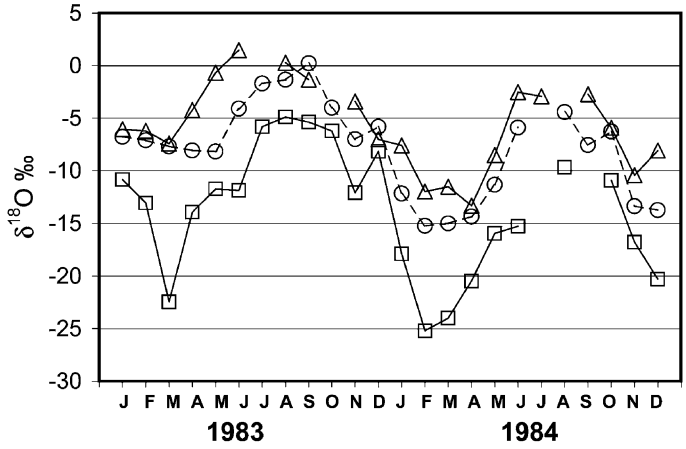

Fig. 3. Seasonal variations of the isotopic composition of precipitation in the Yungas–Altiplano Transect. Triangles: Sapecho, altitude 395 m asl; circles: Sacramento, 2200 m; squares: Chacaltaya, 5200 m.

By combining July and January values, the regression becomes:

$$\delta^2\mathrm{H} = (8.05 \pm 0.09)\,\delta^{18}\mathrm{O} + (11.6 \pm 4.5) \qquad (8)$$

Contrary to the tropics, in the temperate zone the slopes of summer and winter precipitation are both slightly above 8, and winter precipitation is depleted in heavy isotopes with respect to summer rains because temperature is the main isotopic driving factor. Hence, the combination of summer and winter values lowers the slope and brings it close to 8 (Gonfiantini, 1998, 1999). Thus, the $\delta^{18}\mathrm{O}$–$\delta^2\mathrm{H}$ slope appears to change with latitude when precipitation of different seasons are considered separately. The combination of isotopic values of different seasons produces the slope 8, which appears to be constant at the global scale: to some extent, an artifact.

5. The seasonal variations and the isotope amount effect

Due to the so-called amount effect, the heavy isotope content of tropical precipitation is lower during the rainy season than in the dry season. This is clearly shown by the data from the Yungas–Altiplano transect in Bolivia, for which monthly values are available (Fig. 3). In particular, it can be seen that in January and February 1983 affected by drought the δ values were considerably less negative than in the same months in 1984, when precipitation was very abundant. The strong negative isotopic signature of early 1984 can be used for identifying the corresponding ice layer of glaciers in the region and refining the isotopic dating of vertical ice profiles. For instance, the 12‰ sharp $^{18}\mathrm{O}$ decrease observed in the upper part of the Sahama Volcano ice core can be attributed to 1984 precipitation, instead of 1981–1983 as inferred from the profile reported by Thompson et al. (1998).

As broadly speaking the isotope amount effect is a consequence of a Raleigh condensation and rainout process of atmospheric vapour, the correlation between δ values and amount of precipitation is not linear: in principle, it must be steeper, and the ordinate intercept more negative, at high altitude, where precipitation derive from vapour in more advanced stages of condensation. The data confirm this prediction: for the Yungas–Altiplano transect in Bolivia, the slope of the least square regression of $\delta^{18}\mathrm{O}$ on p (rain amount) is $-(0.066 \pm 0.015)$‰ mm^{-1} and the intercept -9.4 ± 1.0‰ for stations above 4000 m asl, and $-(0.014 \pm 0.003)$‰ mm^{-1} and -3.4 ± 0.7‰, respectively, for stations below 1000 m.

An additional reason why at low altitude the slope is less pronounced is the contribution of vapour recycled by evapotranspiration (Salati et al., 1979; Gat and Matsui, 1991), which is important in the Amazon region and decreases at higher altitudes. The system is open: the recycled vapour is isotopi-

cally identical to rainfall and heavier than the vapour left in the system, so counteracting the heavy isotope depletion due to rainout. For comparison, in tropical islands the $\delta^{18}O$ slope is $-0.02‰\ mm^{-1}$ (Rozanski et al., 1993) because of the continuos advection of marine vapour, the effect of which on the isotopic composition of rains is comparable, to some extent, to that of evapotranspiration.

Hence, whenever strong deviations of the rainfall amount from normal occur, often but not necessarily associated with ENSO, they have an impact on the isotopic signature of precipitation. In Ecuador, rains are depleted in heavy isotopes in years affected high rainfall induced by El Niño (García et al., 1998). The same happens in Rio Paraná, South America, whose floods are controlled by ENSO (Depetris et al., 1996). Also the anomalous low $\delta^{18}O$ values of precipitation from November 1997 till April 1998 in Eastern Missouri, USA, was attributed to the ENSO impact (Frederickson and Criss, 1999).

6. The isotopic gradient with altitude

6.1. Observed gradients

The isotopic results show a clear-cut relationship with altitude which closely approaches a linear correlation (Fig. 4). For Mount Cameroon, during the whole sampling period 1972 to 1975, the least square regression between $\delta^{18}O$ mean values and altitude z (in km) is:

$$\delta^{18}O‰ = -(1.56 \pm 0.05)\,z - (3.16 \pm 0.11) \quad (9)$$

Slope and intercept change slightly from one year to another. The extreme values of the slope were $-1.42‰\ km^{-1}$ in 1975 and -1.61 in 1973 and 1974; and those of the intercept -2.65 in 1972 and -3.47 in 1975.

The $\delta^{18}O$–altitude relationships are excellent in the two Bolivian transects as well. The gradient is steeper in rainy years: $-2.39 \pm 0.15‰\ km^{-1}$ in the rainy 1984 vs. -1.48 ± 0.25 in the dry 1983 for the Yungas–Altiplano transect, and -1.60 ± 0.18 in 1985 for the Chaparé–Cochabamba transect. This conclusion is confirmed, in the Yungas–Altiplano transect, by the seasonal changes of the $\delta^{18}O$–altitude monthly gradients, which are steeper in rainy months than in dry months by a factor 2 or even more. For instance, in the exceptionally rainy February 1984, the gradient was -2.62 ± 0.25, while in the relatively dry February 1983, it was -1.53 ± 0.14, and only -1.11 ± 0.12 in August 1983 in full dry season.

Other $\delta^{18}O$ gradients vs. altitude in tropical environments, quoted here for comparison, include $-2.7 \pm 0.3‰\ km^{-1}$ observed in a single snowfall along the slope of Mount Kilimanjaro, Kenya, between 4600 and 5700 m asl (Tongiorgi, 1970), and -1.7 reported for two transects in Ecuador from the Pacific Ocean to the Amazon basin across the Altiplano (García et al., 1998).

Aravena et al. (1989, 1999) reported data on the variation of the stable isotope composition of precipitation with altitude on the Pacific slope of the Andean Cordillera in Northern Chile, east of the desert known as Pampa del Tamarugal (lat. 19–21°S, long. 69°W). The sampling stations had an elevation ranging from 2400 to 4200 m asl. Since the data were obtained on individual rains collected at each station in different days in the time span from 1984 to 1986, the comparison between stations is not straightforward. Notwithstanding, data on summer rains of January–March 1984, together with those reported by Fritz et al. (1981), show, on the whole, a good correlation vs. altitude, but the $\delta^{18}O$ gradient of about $-10\ ‰\ km^{-1}$ seems too high for these latitudes and temperatures. The decreasing content of heavy isotopes vs. altitude, coupled with the increasing precipitation, suggests the occurrence of a second source of moisture from the Pacific. Therefore, this appears to be a pseudo-altitude effect, i.e. not due to the rainout of vapour of a single origin. Winter rains (June 1984 only) and 1986 summer rains do not show any clear relationship between isotopic composition and altitude, which again suggests a multiple-source origin of atmospheric moisture in this region.

The heavy isotope content of precipitation does not decrease always in the same manner with the altitude. Shadow effects may cancel the isotopic variation, as for instance on the western slopes of Mount Kenya (Rietti-Shati et al., 2000). Isotopic data on precipitation in the basin of Mexico do not show a clear trend with altitude; however, at elevation above 3000 m the available $\delta^{18}O$ data indicate

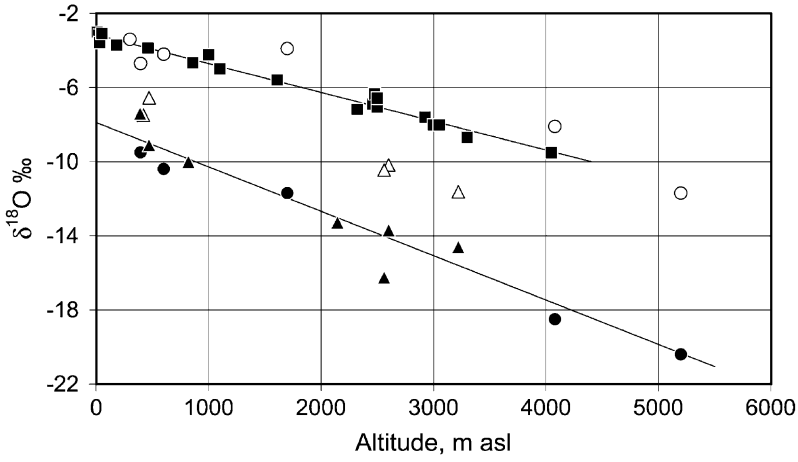

Fig. 4. δ^{18}O–altitude relationships. Filled squares: Cameroon (mean values); open and full circles: Yungas–Altiplano Transect in 1983 and 1984, respectively; full and open triangles: Chaparé–Cochabamba Transect in 1984 and 1985, respectively. The upper line is the linear regression for Cameroon with slope -1.56 ± 0.05‰ km^{-1}, and the lower one that for the two combined Bolivian transects in 1984 with slope -2.39 ± 0.15‰ km^{-1}. The full triangle well below the regression line is the value for Cochabamba in 1984, which deviates from the general relationship possibly because of the shadow effect. Cochabamba is not included in the regression.

an altitude effect of about -2‰ km^{-1} (Cortés et al., 1997).

6.2. Rayleigh condensation process

The variation of rain isotopic composition with altitude can be fitted by a numerical model based on a Raleigh adiabatic condensation process. As already mentioned, Rayleigh models are based on the preferential condensation and removal from the system of isotopically heavy molecules of atmospheric vapour. Adiabatic and isobaric Rayleigh models have been invoked repeatedly to explain the dependency on temperature of the isotopic variations of precipitation and the consequent seasonal, altitude, latitude, continentality effects (Dansgaard, 1964; Jouzel and Merlivat, 1984; Grootes et al., 1989; Gat, 1996 and many others).

The model is described with full mathematical details in Appendix A. In the present study, only the formation of liquid water is considered, which is removed from the system as precipitation (snowfalls are rare and occur only at the highest stations). At temperatures below zero, occurrence of supercooled liquid water is assumed. Ice formation, if occurring, is supposed to take place by freezing the water droplets without affecting the isotopic composition. However, the isotopic fractionation in the subsequent vapour condensation on the ice surface, deviates from the equilibrium value because the light molecules $^{1}H_{2}{}^{16}O$ may be privileged for their higher diffusivity in air (Merlivat, 1978; Jouzel and Merlivat, 1984). This effect tends to offset the thermodynamic equilibrium by which the isotopically heavy molecules are preferentially fixed in condensed phases, and may determine a significant increase of the deuterium excess, because of the relatively small difference in diffusivity coefficients between $HD^{16}O$ and $H_{2}{}^{18}O$.

Finally, the model does not account for contribution of recycled water vapour by evapotranspiration (although this could be easily incorporated in the equations). The model, therefore, is based on a simplified representation of the precipitation process: even so, the relationships vs. altitude z produced by the model match very well the isotopic data, inclusive those on the deuterium excess, as shown by Figs. 5–7.

The fitting parameters are reported in the figure captions. For Cameroon, the lapse rate adopted for the model fitting is -5.3°C km^{-1} as measured by balloons. For Bolivia, the lapse rates used range from -4 (August 1983) to -6.5°C km^{-1} (February 1984), to be compared with the mean temperature

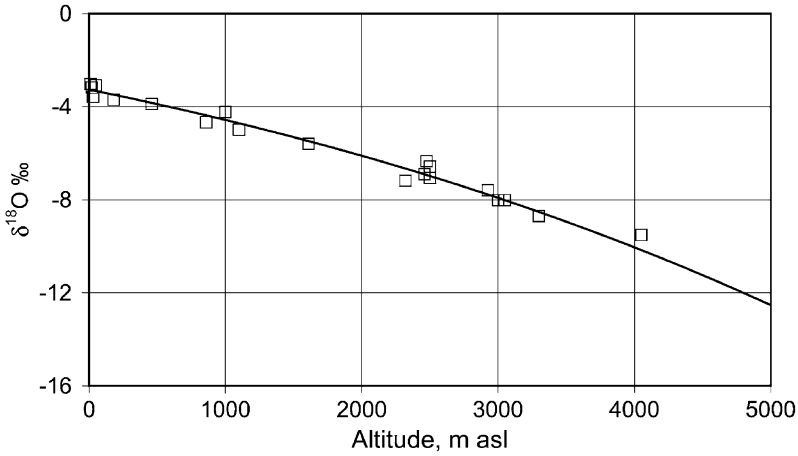

Fig. 5. Mt. Cameroon. Model fitting of precipitation isotopic data (mean interannual values). Fitting parameters: T_0 (air mass initial temperature) 26°C, h_0 (initial relative humidity) 90%, $\delta^{18}O_0$ (initial isotopic composition of atmospheric vapour) −12.6‰, WLR (wet lapse rate) −5.3°C km^{-1}.

gradient at the land surface of −5°C km^{-1}. The $\delta^{18}O$ values adopted for the initial isotopic composition of vapour range from −8.3‰ in the dry August 1983 to −21.9 in the wet February 1984, which are compatible with the spatial distribution of rainfall isotopic composition in the Amazon basin (Salati et al., 1979; Gat and Matsui, 1991; IAEA (International Atomic Energy Agency), 1992).

Hydrogen isotope variations are matched equally well by the model, as it should be expected as a

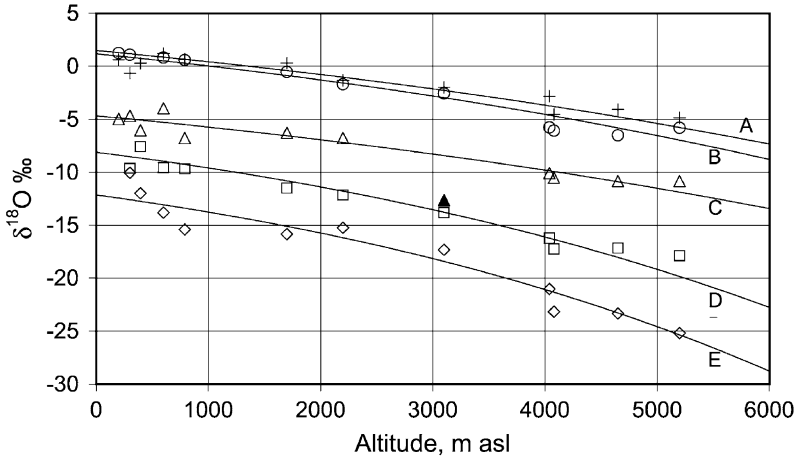

Fig. 6. Bolivia, Yungas–Altiplano Transect. Model fitting of the isotopic composition of monthly precipitation. Crosses and curve A: August 1983 ($h_0 = 80\%$, $\delta^{18}O_0 = -8.3‰$, WLR −4°C km^{-1}); circles and B: July 1983 ($h_0 = 85\%$, $\delta^{18}O_0 = -8.9‰$, WLR −4.5°C km^{-1}); triangles and C: January 1983 ($h_0 = 80\%$, $\delta^{18}O_0 = -14.3‰$, WLR −4.5°C km^{-1}); squares and D: January 1984 ($h_0 = 90\%$, $\delta^{18}O_0 = -17.4‰$, WLR −6°C km^{-1}); lozenges and E: February 1984 ($h_0 = 90\%$, $\delta^{18}O_0 = -21.9‰$, WLR −6.5°C km^{-1}). The full triangle represents the January 1983 value for Chuspipata, which clearly deviates from the general trend. (See caption of Fig. 5 for the explanation of fitting parameters.) $T_0 = 26$°C in all cases.

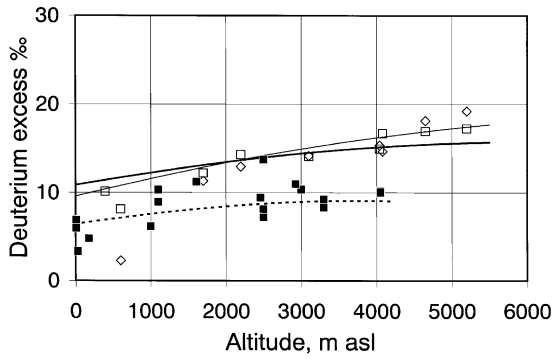

Fig. 7. Model fitting of the deuterium excess values. Cameroon: filled squares (data) and dotted line (model). Bolivia, Yungas–Altiplano Transect: January 1984, open squares and thick line; February 1984, lozenges and thin line.

consequence of the correlation between hydrogen and oxygen isotope compositions.

It is possible that monthly and annual mean values of the isotopic composition of precipitation, as used in this study, obey better the Rayleigh condensation model than those of individual precipitation events. In fact, monthly and annual values tend to average the formation conditions of precipitation and smooth off irregularities, deviations from the general trend, and noises due to local occurrences. Therefore, monthly and annual samples appear adequate to investigate the mean major features of processes producing precipitation, especially in regular precipitation regimes as in the two cases described here.

7. Conclusions

In tropical regions, the altitude effects on the isotopic composition of precipitation can be adequately described in terms of a Rayleigh adiabatic condensation process of the atmospheric vapour. This implies that the vapour derives from a single source, as for Mt. Cameroon and Bolivia cases discussed in this paper.

The slope of the isotopic composition of precipitation vs. altitude and the initial isotopic composition of atmospheric vapour change seasonally and appear to be related to the amount of precipitation: in wet months the isotopic gradient vs. altitude is larger than in dry months. Model computations, based on a Rayleigh condensation process of atmospheric vapour to liquid water under isotopic equilibrium conditions, confirm these findings, and indicate that the main reason is the apparent larger wet lapse rate (temperature vertical gradient) in rainy months. In addition, the model explains the observed increase of the deuterium excess with altitude.

In Bolivia, the $\delta^2H/\delta^{18}O$ regression slopes are about 7.5 when summer (rainy season) and winter (dry season) are considered separately, and the intercept is higher in winter than in summer, as usual. However, in the tropics, the heavy isotope content of precipitation is higher in the dry than in the rainy season, because it is governed by the amount of precipitation. Thus, the well-known slope 8, typical of the world meteoric water line, is obtained by combining summer and winter precipitation.

Acknowledgements

Prof. Jean-Charles Fontes passed away in February 1994 in a car accident during a field mission to Mali, Africa. His keen interest and suggestions greatly contributed to design the work programme described in this paper. Without his support, the data reported here probably would not exist.

Thanks are due to Prof. Kazimierz Rozanski, Institute of Physics and Nuclear Techniques, Cracow, Poland, for his careful reading the manuscript, and for criticisms and suggestions which greatly improved it. Useful remarks from another unknown reviewer are also acknowledged.

Finally, the senior author would like to thank colleagues and friends from the Laboratoire de Hydrologie et de Géochimie Isotopique, Université de Paris Sud, Orsay, where he spent a period of 6 months in 1995. This work was mainly conceived during that time.

Appendix A. The Rayleigh adiabatic condensation of water vapour

When an air mass rises and expands adiabatically due to the pressure decrease, it goes through the following subsequent steps: (i) the air mass cools

down until it reaches the water vapour saturation; (ii) the water vapour starts to condense and form liquid water (or ice), i.e. to build up clouds; and (iii) part of the condensed phase is removed from the system as precipitation. The physico-chemical relationships governing these processes are reported below.

The cooling gradient with altitude is greater during the 'dry' adiabatic cooling, i.e. before condensation starts. During condensation, the latent heat of vaporization is released into the system, with the consequent slowing down of the cooling rate. If part of the water or ice formed is removed by precipitation, the process becomes pseudo-adiabatic, because a small part of the system energy is removed as well. However, this energy loss is minimal and could be neglected in the first approximation.

A.1. Before water vapour saturation is attained

The energy variation dE of an air mass undergoing adiabatic expansion is:

$$dE = (nC_{PA} + m_0C_{PV})dT - (n + m_0)RT\frac{dP}{P} = 0 \quad (A1)$$

where C_{PA} and C_{PV} are the molar heat capacity of dry air and water vapour at constant pressure, respectively; n and m_0 are the moles of dry air and water vapour present in the system, respectively; P is the pressure, and dT and dP are the temperature and the pressure variations.

Before saturation is attained, the water vapour amount in the system does not change. Therefore:

$$\frac{m_0}{n + m_0} = \frac{P_V}{P} = \frac{hP_S}{P} \quad (A2)$$

where h is relative humidity, P_V is the vapour partial pressure and $P_S = P_S(T)$ is the vapour saturation pressure at the temperature T and pressure P of the system.

For example, assuming as initial conditions at ground level (i.e., at the moment in which the air mass leaves the contact with the sea surface) that the temperature is 26°C, the pressure is 1 atm, and the relative humidity is 80%, the saturation is attained at about 21.5°C, i.e. at an altitude between 500 and 800 m.

A.2. After water vapour saturation is attained

When, as a consequence of cooling, the vapour partial pressure of the air mass attains the saturation value, condensation of liquid water starts to take place. Ice may be formed at temperatures below 0°C; frequently, however, supercooled water is formed. In this treatment, we consider that the condensed phase is formed by liquid water only.

The material balance is:

$$dm + dw + dp = 0 \quad (A3)$$

and the energy budget:

$$(nC_{PA} + mC_{PV} + wC_L)dT - (n + m)RT\frac{dP}{P} + H_V dm + H_L(dw + dp) = 0 \quad (A4)$$

In the above equations dm is the condensing vapour, w and dw are the co-existing liquid water in the system and its variation, and $dp = -(dm + dw)$ is water removed by precipitation. H_V is the molar heat of vaporization of liquid water, C_L is the molar heat capacity of liquid water saturated with air, assumed to be constant in the range of temperature considered, and $H_L = C_L(T–273.15)$ is the liquid water enthalpy. If $dp > 0$, i.e. if precipitation occurs, a small fraction of energy, equal to $-H_L dp$, is removed from the system, which becomes pseudo-adiabatic. In addition, if $w > 0$, the condensation becomes a pseudo-Rayleigh process, because in a Rayleigh process only one phase is present and all the liquid formed is removed.

Using Eq. (A3), Eq. (A4) becomes:

$$(nC_{PA} + mC_{PV} + wC_L)dT - (n + m)RT\frac{dP}{P} + (H_V - H_L)dm = 0 \quad (A5)$$

After saturation is attained ($h = 1$), Eq. (A2) becomes:

$$\frac{m}{n + m} = \frac{P_S}{P} \quad (A6)$$

$$dm = \frac{n(PdP_S - P_S dP)}{(P - P_S)^2} \quad (A6')$$

Using the above relationships, Eq. (A5) can be rewritten as:

$$\mathrm{d}m = \frac{nC_{\mathrm{PA}} + mC_{\mathrm{PV}} + wC_{\mathrm{L}} - (n+m)RT\dfrac{\mathrm{d}P_{\mathrm{S}}}{P_{\mathrm{S}}\mathrm{d}T}}{H_{\mathrm{V}} - H_{\mathrm{L}} + \dfrac{nRT}{m}}\mathrm{d}T \tag{A7}$$

$$\mathrm{d}P = \frac{P}{(n+m)\left(H_{\mathrm{V}} - H_{\mathrm{L}} + \dfrac{nRT}{m}\right)} \times \left[\frac{n}{m}(nC_{\mathrm{PA}} + mC_{\mathrm{PV}} + wC_{\mathrm{L}}) + (n+m)(H_{\mathrm{V}} - H_{\mathrm{L}})\frac{\mathrm{d}P_{\mathrm{S}}}{P_{\mathrm{S}}\mathrm{d}T}\right]\mathrm{d}T \tag{A8}$$

Note that T is kept here as main independent variable, which is convenient because P_{S} and α (the isotopic fractionation factor between liquid and vapour, see Section A.5) depend on temperature only. In addition, the wet lapse rate (vertical temperature gradient after saturation is attained) can be assumed as linear:

$$\mathrm{d}T/\mathrm{d}z = a \tag{A9}$$

and therefore variations of temperature can be easily converted in terms of altitude variations.

A.3. Rayleigh and pseudo-Rayleigh condensation

Eqs. (A7) and (A8) enable numerical computations. In the most simple case of a Rayleigh type process, in which the liquid phase formed by vapour condensation is assumed to be totally removed from the system as precipitation, the term wC_{L} in the equations above vanishes, being $w = 0$ and $\mathrm{d}m = -\mathrm{d}p$ always. The process is pseudo-adiabatic.

Eqs. (A7) and (A8) can be used also if part of the condensed phase remains in the system. Let consider here the two following cases.

(i) Only a fraction of the condensed water precipitates as rain, and the ratio w/m between condensed phase and vapour in the air mass increases steadily with altitude. If x is the precipitating fraction, we have $\mathrm{d}p = -x\mathrm{d}m$ and $\mathrm{d}w = -(1-x)\mathrm{d}m$. The process is pseudo-adiabatic and pseudo-Rayleigh.

(ii) No precipitation takes place till the ratio w/m between condensed phase and vapour in the air mass has attained the value X. Therefore, when $w/m < X$, we have $\mathrm{d}p = 0$, $\mathrm{d}w = -\mathrm{d}m$, and $w = m_0 - m$ the process is adiabatic.

If we assume that the ratio w/m remains constant and equal to X, once this value is attained, and the condensed phase in excess is removed by precipitation, we have: $\mathrm{d}w = X\mathrm{d}m$ and $\mathrm{d}p = -(1+X)\mathrm{d}m$. Note that, as the amount of vapour m decreases, the amount of precipitation exceeds that of vapour condensed in each cooling step.

A.4. The isotopic composition of precipitation

Isotopic equilibrium is assumed to occur between vapour and the liquid phase formed at any condensation step, and between vapour and the co-existing liquid phase in clouds. The isotopic composition of precipitation is equal to that of the liquid phase. Thus:

$$\frac{1000 + \delta_{\mathrm{L}}}{1000 + \delta_{\mathrm{V}}} = \alpha_{\mathrm{LV}} \tag{A10}$$

where α_{LV} is the liquid–vapour isotope fractionation factor that depends only on temperature.

The material balance equation is:

$$m_{i+1}\delta_{\mathrm{V}(i+1)} + w_{i+1}\delta_{\mathrm{L}(i+1)} + p_{i+1}\delta_{\mathrm{L}(i+1)} = m_i\delta_{\mathrm{V}i} + w_i\delta_{\mathrm{L}i} \tag{A11}$$

where m and w respectively represent the amounts of vapour and liquid water present in system in condensation steps i and $i+1$, and p_{i+1} the amount of rain formed in step $i+1$. By combining (A10) and (A11) we obtain, for the residual vapour after the condensation step $i+1$:

$$\delta_{\mathrm{V}(i+1)} = \frac{m_i\delta_{\mathrm{V}i} + w_i\delta_{\mathrm{L}i} - 1000(\alpha_{\mathrm{LV}(i+1)} - 1)(w_{i+1} + p_{i+1})}{\alpha_{\mathrm{LV}(i+1)}(w_{i+1} + p_{i+1}) + m_{i+1}} \tag{A12}$$

When ice is formed, the fractionation factor to be considered in the condensation process is that between ice and vapour. The process, however, becomes complex for the possible lack of equilibrium due to the different diffusivity of isotopic molecules in air, as already discussed, and the slowdown of the isotopic re-equilibration between vapour and ice

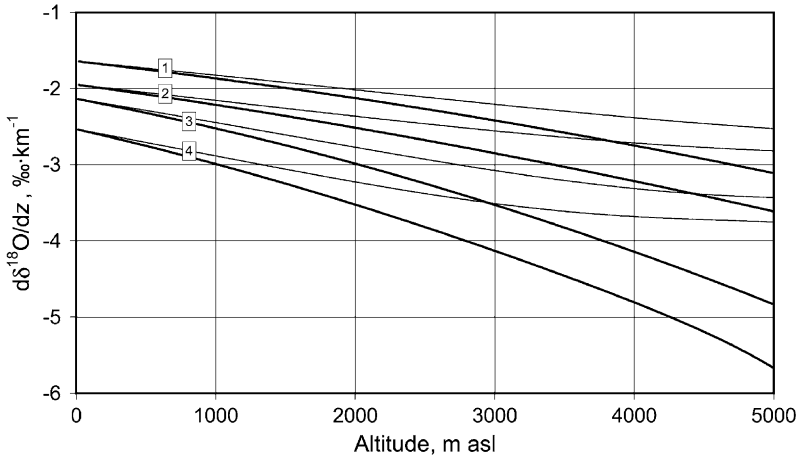

Fig. 8. Model variation of the $\delta^{18}O$ gradient vs. altitude. Thick curves show the pure Rayleigh process (liquid water is fully removed by precipitation), and thin curves depict the pseudo-Rayleigh process (with $x = 0.85$, i.e. 15% of the water condensed at each step remains in the system and co-exists with vapour). Curves 1: $h_0 = 80\%$, HLR -5°C km^{-1}; curves 2: $h_0 = 60\%$, HLR -5°C km^{-1}; curves 3: $h_0 = 80\%$, HLR -6.5°C km^{-1}; curves 4: $h_0 = 60\%$, HLR -6.5°C km^{-1}.

crystals in clouds. In this paper, the ice occurrence is not considered in modelling the condensation process.

A.5. Values of parameters

In this section, we report the values of the parameters appearing in Eqs. (A1–12) when used for numerical integrations. The parameters are either considered constant or function of temperature only, at the conditions of pressure and temperature experienced by the air mass.

The relationship between the vapour saturation pressure P_S (in Pa) and temperature (in K) for liquid water is obtained by the polynomial fitting of P_S values between 30°C and -16°C:

$$P_S = 2.570526 \times 10^{-6} T^5 - 3.216966 \times 10^{-3} T^4 + 1.623244 T^3 - 4.124816 \times 10^2 T^2 + 5.274678 \times 10^4 T - 2.713693 \times 10^6$$

$$dP_S/dT = 1.28526 \times 10^{-5} T^4 - 1.28679 \times 10^{-2} T^3 + 4.86973 T^2 - 8.24963 \times 10^2 T + 5.27468 \times 10^4$$

$$C_{PA} = 29.083\ \text{J mol}^{-1}\ \text{K}^{-1}\ (\text{dry air})$$

$$C_{PV} = 35.136\ \text{J mol}^{-1}\ \text{K}^{-1}\ (\text{vapour})$$

H_V and H_L depend linearly on temperature and C_L is constant:

$$H_V = 43{,}854.18 - 39.31 \times (T - 298.16)\ \text{J mol}^{-1}$$

$$C_L = 75.450\ \text{J mol}^{-1}\ (\text{at } 0\text{°C})$$

$$H_L = C_L \times (T - 273.16)\ \text{J mol}^{-1}$$

$R = 8.3114$ J mol^{-1} K^{-1} (value for humid air, interpolated from the values of dry air and water vapour).

The isotope fractionation factors between liquid water and vapour are computed by using the equations below (Majoube, 1971):

$$\ln \alpha(^{18}O)_{LV} = 1137 T^{-2} - 0.4156 T^{-1} - 0.00207$$

$$\ln \alpha(^{2}H)_{LV} = 24{,}844 T^{-2} - 76.248 T^{-1} + 0.05261$$

where the temperature is expressed in K. Majoube's equations have been derived for the temperature interval 0–100°C, but are used here also for temperature up to -10°C.

For the isotopic equilibrium ice–vapour, the liquid fractionation factors above should be multiplied by the ice–liquid fractionation factors: $\alpha_{IV} = \alpha_{LV}\alpha_{IL}$. The equilibrium fractionation factors between ice and liquid water are (O'Neil, 1968):

$$\alpha(^{18}O)_{IL} = 1.0031$$

$$\alpha(^{2}H)_{IL} = 1.0195$$

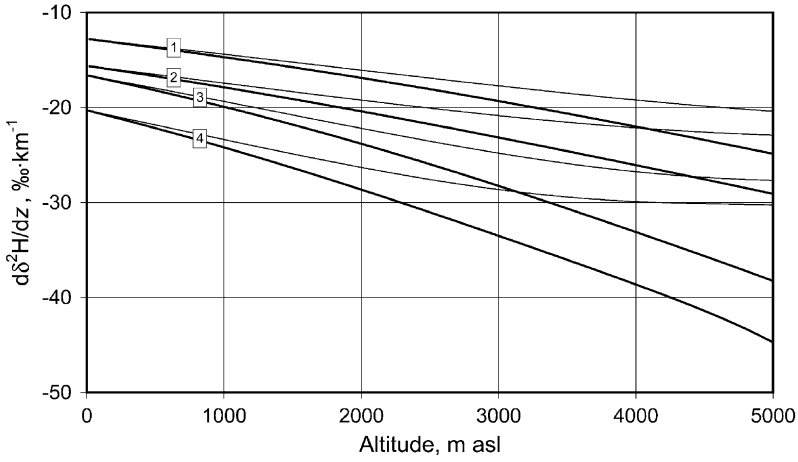

Fig. 9. Model variation of the δ^2H gradient vs. altitude. Parameters as in Fig. 8.

In addition, if ice occurs, the term of the latent heat of fusion (6007.7 J mol^{-1} at 0°C) must be added to the above vaporization heat H_V, the molar heat of ice (37.942 J mol^{-1} at 0°C) should be used for C_L, and the relationship between saturated vapour pressure and temperature must be changed accordingly.

A.6. Computer simulations

Computer simulations are illustrated by Figs. 8–10. The altitude $z = 0$ is that at which the first precipitation occurs: in case of a Rayleigh process ($x = 0$), this corresponds to the saturation attainment of the rising air mass.

The δ^{18}O gradient vs. temperature predicted by the model ranges from 0.38‰/°C to 0.64‰/°C in the temperature range 10°C to −10°C (initial relative humidity 80%), to be compared with the values of 0.62‰/°C reported by Rozanski et al. (1993) for mid latitude stations, and 0.42‰/°C for summer rains and 0.58‰/°C for winter precipitation reported by Fricke and O'Neil (1999).

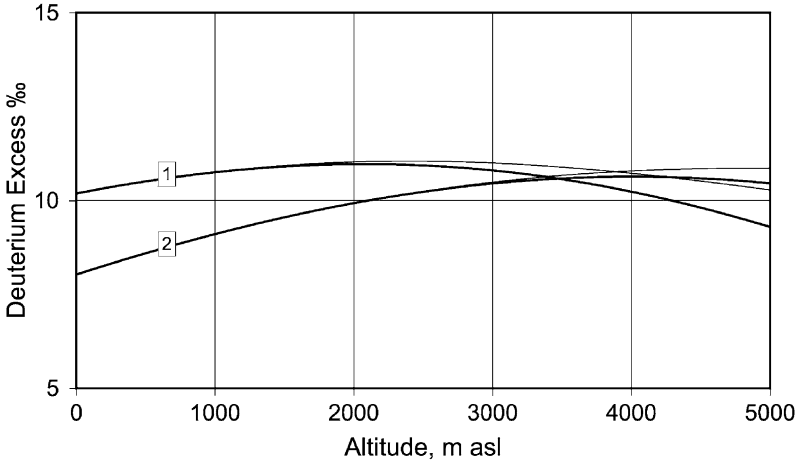

Fig. 10. Model deuterium excess variation vs. altitude in a pure Rayleigh process. Thick curves: HLR $-5°C \cdot km^{-1}$; thin curves: HLR $-6.5°C\ km^{-1}$. Curves 1: $h_0 = 60\%$; curves 2: $h_0 = 80\%$.

The isotopic gradient of precipitation vs. altitude (i.e., with decreasing temperature) predicted by the model, is shown in Figs. 8 and 9. The curves slightly deviates from linearity (as already shown in Figs. 6 and 7). The bending depends mainly on the wet lapse rate dT/dz and, to a lesser degree, the relative humidity h of the rising air mass. Changing the vapour initial isotopic composition δ_0 only shifts vertically the curve.

The isotopic gradient becomes steeper from 0- to 5000-m elevation by a factor 1.5–2 depending on the values selected for dT/dz and h, which eventually does not produce a large deviation from the linear trend. The increasing isotopic gradient with altitude is caused by the increase of the relative vapour condensation rate as temperature decreases. However, if part of the water formed remains in the clouds and co-exists with the vapour, the isotopic gradient increase with altitude is less marked, and the same happens if recycling of water vapour takes place. Incidentally, the fact that the gradient $d\delta/dz$ is larger at low temperature implies that the altitude effect on the isotopic composition of precipitation should increase with latitude.

Fig. 10 shows that the deuterium excess tends to increase with altitude if the initial relative humidity is 80% or more, while it does not vary much when relative humidity is 60% or less (which implies a lower condensation temperature). The trend illustrated refers to Rayleigh conditions, but it does not change significantly with co-existing liquid and vapour. It should be noted however that the deuterium excess variations depend strongly on the isotopic fractionation factors, which may not be adequately represented by Majoube's equations at temperatures below zero.

References

Aravena, R., Peña, H., Grilli, A., Suzuki, O., Mordeckai, M., 1989. Evolución isotópica de las lluvias y origen de las masas de aire en el Altiplano chileno. Estudios de Hidrología Isotópica en América Latina. IAEA-TECDOC-502. IAEA, Vienna, pp. 129–142.

Aravena, R., Suzuki, O., Peña, H., Pollastri, A., Fuenzalida, H., Grilli, A., 1999. Isotopic composition and origin of the precipitation in Northern Chile. Appl. Geochem. 14, 411–422.

Ardanuy, P.E., Cuddapah, P., Kyle, H.L., 1987. Remote sensing of water vapor convergence, deep convection, and precipitation over the tropical Pacific Ocean during the 1982–1983 El Niño. J. Geophys. Res. 92, 14204–14216.

Cortés, A., Durazo, J., Farvolden, R.N., 1997. Studies of isotopic hydrology of the basin of Mexico and vicinity: annotated bibliography and interpretation. J. Hydrol. 198, 346–376.

Craig, H., 1961. Isotopic variations in meteoric waters. Science 33, 1702–1703.

Dansgaard, W., 1964. Stable isotopes in precipitation. Tellus 16, 436–468.

Depetris, P.J., Kempe, S., Laif, M., Mook, W.G., 1996. ENSO-controlled flooding in the Paraná River (1904–1991). Naturwissenschaften 83, 127–129.

Fontes, J.-Ch., Olivry, J.C., 1976. Gradient isotopique entre 0 et 4000 m dans les précipitations du Mont Cameroun. C.R. Reun. Annu. Sci. Terre, Soc. Géol. France, Paris, 171.

Fontes, J.-Ch., Olivry, J.C., 1977. Composition isotopique des précipitations de la région du Mont Cameroun. ONAREST, Inst. de Recherches sur les Techniques, l'Industrie et le Sous-sol 28 pp.

Frederickson, G.C., Criss, R.E., 1999. Isotope hydrology and residence times of the unimpounded Meramec River Basin, Missouri. Chem. Geol. 157, 303–317.

Fricke, H.C., O'Neil, J.R., 1999. The correlation between $^{18}O/^{16}O$ ratios of meteoric water and surface temperature: its use in investigating terrestrial climate change over geologic time. Earth Planet. Sci. Lett. 170, 181–196.

Fritz, P., Suzuki, O., Silva, C., Salati, E., 1981. Isotope hydrology of groundwaters in the Pampa del Tamarugal, Chile. J. Hydrol. 53, 161–184.

Gaita, A., 1999. Communication presented at the 1st International Course on Isotope Limnology, Puno, Peru, 12–23 April 1999.

García, M., Villalba, F., Araguás Araguás, L., Rozanski, K., 1998. The role of atmospheric circulation patterns in controlling the regional distribution of stable isotope contents in precipitation. Preliminary results from two transects in the Ecuadorian Andes. Isotope Techniques in the Study of Environmental Changes. IAEA, Vienna, pp. 127–140.

Gat, J.R., 1996. Oxygen and hydrogen isotopes in the hydrological cycle. Annu. Rev. Earth Planet. Sci. 24, 225–262.

Gat, J.R., Matsui, E., 1991. Atmospheric water balance in the Amazon Basin: an isotopic evapotranspiration model. J. Geophys. Res. 96, 13179–13188.

Goldberg, R.A., Tisnado, M., Scofield, G., 1987. Characteristics of extreme rainfall events in northwestern Peru during the 1982–1983 El Niño period. J. Geophys. Res. 92, 14225–14241.

Gonfiantini, R., 1998. On the isotopic composition of precipitation. Hydrologie et Géochimie Isotopique. In: Causse, C., Gasse, F. (Eds.), 1998. Proc. Int. Symposium in memory of J.-Ch. Fontes, Paris, June 1995, Orstom, Paris, pp. 3–22.

Gonfiantini, R., 1999. Investigating the hydrological cycle with environmental isotopes. Actas II Simposio Sudamericano de Geología Isotópica, Córdoba, Argentina, 12–16 September 1999, pp. 537–547.

Grootes, P.M., Stuiver, M., Thompson, L.G., Mosley-Thompson, E., 1989. Oxygen isotope changes in tropical ice, Quelccaya, Peru. J. Geophys. Res. 94, 1187–1194.

IAEA (International Atomic Energy Agency), 1992. Statistical treatment of data on environmental isotopes in precipitation. Technical reports series no. 331. IAEA, Vienna.

Jouzel, J., Merlivat, L., 1984. Deuterium and oxygen 18 in precipitation: modeling of the isotopic effects during snow formation. J. Geophys. Res. 89, 11749–11757.

Majoube, M., 1971. Fractionnement en oxygène-18 et en deutérium entre l'eau et sa vapeur. J. Chim. Phys. 197, 1423–1436.

Merlivat, L., 1978. Molecular diffusivities of $H2^{16}O$, $HD^{16}O$ and $H_2{}^{18}O$ in gases. J. Chem. Phys. 69, 2861–2864.

NOAA (National Oceanic and Atmospheric Administration), 1983. Monthly Climatic Data for the World, vol. 36. NOAA, Asheville, NC, USA, (Sponsored by the World Meteorological Organization).

NOAA (National Oceanic and Atmospheric Administration), 1984. Monthly Climatic Data for the World, vol. 37. NOAA, Asheville, NC, USA, (Sponsored by the World Meteorological Organization).

O'Neil, J.R., 1968. Hydrogen and oxygen isotope fractionation between ice and water. J. Phys. Chem. 72, 3583–3584.

Rietti-Shati, M., Yam, R., Karlen, W., Shemesh, A., 2000. Stable isotope composition of tropical high-altitude fresh-waters on Mt. Kenya, Equatorial East Africa. J. Chem. Geol. 166, 341–350.

Roche, M.A., Fernandez, C., 1988. Water resources, salinity and salt exportation of the rivers of the Bolivian Amazon. J. Hydrol. 101, 305–331.

Roche, M.A., Rocha, N., 1985. Mapa Pluviométrico de Bolivia y Regiones Vecinas. PHICAB, La Paz.

Roche, M.A., Bourges, J., Cortes, J., Mattos, R., 1992. Climatology and hydrology of the Lake Titicaca basin. In: Dejoux, C., Iltis, A. (Eds.), Lake Titicaca. Kluwer Academic Publishing, Dordrecht, The Netherlands, pp. 63–68.

Roche, M.A., Gonfiantini, R., Fontes, J.-Ch., Abasto, N., Noriega, L., 1999. The isotopic composition of precipitation on the Andes and Amazon of Bolivia. Isotope Techniques in Water Resources Development and Management. IAEA, Vienna.

Ronchail, J., 1989. Climatological winter effects of southern advections in Bolivia and North-West Brazil (73–84). Proc. 3rd Int. Conf. on Southern Hemisphere Meteorology and Oceanography, Buenos Aires, 13–17 Nov. 1989. Amer. Meteor. Soc., Boston, pp. 180–182.

Rozanski, K., Araguás, L., Gonfiantini, R., 1993. Isotopic patterns in modern global precipitation. In: Swart, P.K., Lohmann, K.C., McKenzie, J., Savin, S. (Eds.), Climatic Changes in Continental Isotopic Records. Am. Geophys. Union, Geophys. Monogr., vol. 78, American Geophysical Union, Washington, DC, pp. 1–36.

Salati, E., Dall'Olio, A., Matsui, E., Gat, J.R., 1979. Recycling of water in the Amazon Basin: an isotopic study. Water Resour. Res. 15, 1250–1258.

Thompson, L.G., Davis, M.E., Mosley-Thompson, E., Sowers, T.A., Henderson, K.A., Zagorodnov, V.S., Lin, P.-N., Mikhalenko, V.N., Campen, R.K., Bolzan, J.F., Cole-Day, J., Francou, B., 1998. A 25,000-year tropical climate history from Bolivian ice cores. Science 282, 1858–1864.

Tongiorgi, E., 1970. "Isotope Hydrology 1970". IAEA, Vienna, pp. 43–57. Reported by R. Gonfiantini in the discussion of H. Moser and W. Stichler: Deuterium measurements on snow samples from the Alps.

WMO/OMM, 1996. Climatological normals (Clino) for the period 1961–1990. WMO/OMM no. 847, Geneva.